CHAPTER IV
SCR ACTIVITY STUDY OF IRON-LOADED MFI ZEOLITE

4.1 ABSTRACT

Fe-MFI zeolite was successfully synthesized using silatrane precursor and tetrapropyl ammonium bromide (TPA) template via sol-gel process and microwave technique. The effects of aging time, heating temperature, heating time and iron concentration were investigated, and it was found that Fe-MFI synthesis favored a higher heating temperature, but was limited by the degradation of a template molecule. Moreover, the longer aging and heating times promote the higher amount of iron atom into MFI structure. However, too long aging time decreases the incorporation of iron. The higher Si/Fe ratio provides the more percentage of Fe^{3+} ions incorporated into MFI framework. The catalytic properties of Fe-MFI catalyst were studied in the selective catalytic reduction (SCR) of NO using CO as a reducing gas, and it was found that the synthesized Fe-MFI zeolite could not catalyze the reduction reaction of SCR of NO by CO. Instead, these catalysts could catalyze the oxidation of CO in this reaction.

Keywords: Fe-loaded MFI zeolite, Sol-gel process, SCR of NO and CO

4.2 INTRODUCTION

Synthesis of Fe-MFI zeolite has gained great interest in view of their excellent catalytic performance [1]. However, iron in the zeolite framework was appeared only in the directly synthesized method [2]. Wongkasemjit et al [3-4] had found a way to synthesize MFI zeolite via the sol-gel process and microwave technique using silatrane and either tetrapropyl ammonium bromide (TPA) or tetrabutyl ammonium bromide (TBA) as a precursor and a template, respectively. They also found that the tendency for MFI formation could be improved by increasing the aging and heating times.

Reduction of NO_x is of great importance and interest in air pollution control, especially, in a high temperature combustion process in automobile engines.

Generally, NO is the major emission gas in these processes [8]. However, CO is also found in ineffective combustion processes. The catalytic reduction of NO in the presence of CO has been widely studied [8], and it can be catalyzed by precious metals dispersed on various supports, such as, Pd on Al_2O_3 [5]. However, due to the scarcity and high cost of these precious metals, Fe-MFI zeolite catalysts are of increasing importance in catalytic reduction of NO.

In this work, iron loaded-MFI zeolite was synthesized using synthesized silatrane as zeolite synthesis precursor and alkaline base as a hydrolysis agent and source of metal ion via the sol-gel process, followed by microwave technique. Influence of the preparation method on the catalytic activity in the reduction of NO using CO as a reductant gas was investigated.

4.3 EXPERIMENTAL

4.3.1 Materials

Fumed silica (SiO_2) and iron (III) chloride ($FeCl_3$) were supplied from Aldrich Chemical. Ethylene glycol ($HOCH_2CH_2OH$) as reaction solvent was obtained from J.T. Baker. Triethanolamine (TEA, $N[CH_2CH_2OH]_3$) was purchased from Labscan. Sodium hydroxide (NaOH) was purchased from EKA Chemicals. Tetrapropyl ammonium bromide (TPA) was obtained from Fluka Chemical AG. All chemicals were used as received. Acetonitrile (CH_3CN) was obtained from Lab-scan Co., Ltd. and distilled prior to use. Nitric Oxide (NO) 1.52% in helium was supplied from Air Products and Chemicals Co., Ltd. Carbon monoxide (CO) 24.85% in helium was supplied from Thai Industrial Gases (Public) Co., Ltd. Oxygen (O_2) 21.30% in helium was supplied from Praxair (Thailand) Co., Ltd. High purity helium was supplied from Thai Industrial Gases (Public) Co., Ltd.

4.3.2 Instrumentation

FTIR spectroscopic analysis was conducted using a Bruker Instrument (EQUINOX55) with 2 cm^{-1} resolution. The solid samples were mixed and palletized with dried KBr. Thermo gravimetric analysis (TGA) was carried out on a Perkin

Elmer TGA7 at a scanning rate of 10°C/min under nitrogen atmosphere. The crystal morphology was studied using a JEOL 5200-2AE scanning electron microscope (SEM). Crystal structure was characterized using a Rigaku X-ray diffractometer (XRD) at scanning speed of 5°/sec using CuKα as incident radiation and a filter. The working range was 3°-50° θ/2θ with 1°, 0.3 mm setting of divergent, scattering and receiving slit, respectively. UV-visible measurement was performed on Shimadzu UV-2550 with the ISR-2200 integrating sphere attachment, using $BaSO_4$ as reference sample. The Si/Fe ratio was determined by X-ray fluorescence (XRF) spectroscopy (Bruker model SRS 3400). Electron spin resonance (ESR) spectroscopy was measured at X-band, ~9 GHz, on a ESPRIT-425 vol.604 spectrometer.

4.3.3 Catalyst Preparation Procedure

4.3.3.1 Silatrane Synthesis (Si-TEA) [6]

Silatrane (tris(silatranyloxyethyl) amine or SiTEA) was synthesized by heating a mixture of TEA (0.125 mol), SiO_2 (0.1 mol) and EG (100 mL) at 200°C under nitrogen atmosphere. The reaction was complete within 10 h, and the mixture was cooled to room temperature before distilling off the excess EG under vacuum (8 mmHg) at 110°C. The brownish white solid was washed three times with dried acetonitrile to obtain a fine white powder. The silatrane product was characterized using XRD, TGA and FTIR.

4.3.3.2 Fe-MFI Synthesis [3-4]

Silatrane and TPA were dispersed in water using the SiO_2:0.1TPA:0.4NaOH:144H_2O: 0.01$FeCl_3$ formula, and continuously stirred before adding iron (III) chloride. Stoichiometric amount of sodium chloride was further added into the mixture. To establish the optimum reaction conditions for the ratio of Si/Fe equal to 100 in the gel, the effects of aging time, heating time and heating temperature were studied. Additionally, the effect of the Si/Fe ratio was also studied by varying the ratio from 100 to 19. The as-synthesized Fe-MFI products were calcined in an electronic furnace set at 550°C with the heating rate of 0.5°C/min. The calcined products were characterized using XRD, SEM, DR-UV, XRF and ESR.

4.3.4 Apparatus

Figure 4.1 shows the schematic flow diagram of catalytic activity study. In this work, the experimental apparatus was divided into 3 sections: (i) gas blending system (ii) catalytic reactor and (iii) analytical instrument.

4.3.4.1 Gas Blending System

The reactant mixture was consisted of 0.1% nitric oxide, 1% carbon monoxide and 0.45% oxygen balanced in helium. To obtain a desired component of the typical reactant mixture, a mass flow controller (Sierra Instrument, Inc. model 840) was applied to control the flow rate of each reactant gas. The reactant mixture was passed through a check valve to protect reverse flow before being passed to the reactor.

4.3.4.2 Catalytic Reactor

The activity of synthesized catalyst was carried out using the selective catalytic reduction of NO reaction. Catalyst (200 mG) was packed in the middle of a 1 cm outside diameter borosilicate glass reactor containing glass wool. The experiment was performed at atmospheric pressure with the space velocity of 42,000 h^{-1}. The reaction temperature studied was ranged from 323 to 723 K which was controlled by PID controller equipped with K-type thermocouple (Yokohama, Model UP27). The final product gas was detected using analytical instruments.

4.3.4.3 Analytical Instruments

The effluent gas was analyzed both quantitatively and qualitatively. A product gas from the reactor was splitted into two parts. First, O_2 and N_2 mixture concentration was determined using Hewlett Packard 3365 series II Chemstation with a molecular sieve 13X column. The other part of the product gases were passed to the high level Chemiluminescence NO-NO_2-NO_x analyzer of ECO physics Model CLD 700 EL to determine nitric oxide (NO) and nitrogen oxide (NO_2) concentration. In addition, the concentration of N_2O was calculated from mass balance.

4.4 RESULTS AND DISCUSSION

4.4.1 Silatrane characterization

Following the method of Wongkasemjit [6], silatrane was synthesized directly from inexpensive and widely available starting materials, SiO_2 and TEA, via the Oxide One Pot Synthesis (OOPS) process. The white product was characterized using FTIR and TGA.

From Figure 4.2, FT-IR bands observed were 3000-3700 cm^{-1} (w, intermolecular hydrogen bonding), 2860-2986 cm^{-1} (s, νC-H), 1244-1275 cm^{-1} (m, νC-N), 1170-1117 (bs, νSi-O), 1093 (s, νSi-O-C), 1073 (s, νC-O), 1049 (s, νSi-O), 1021 (s, νC-O), 785 and 729 (s, νSi-O-C) and 579 cm^{-1} (w, Si<---N). TGA shows one sharp mass loss transition at 390°C, as seen from Figure 4.3 with 19% ceramic yield corresponding to $Si((OCH_2CH_2)_3N)_2H_2$ having the theoretical yield of 18.58%.

4.4.2 Fe-MFI characterization

In this work, TPA was used as the template for producing Fe-MFI. Following the previous studies [3-4], the formulation was SiO_2:0.1TPA:0.4NaOH:144H_2O for producing small and perfect MFI crystals. To load Fe into the MFI structure, it was necessary to investigate the effects of these parameters, viz. aging time, heating temperature, heating time and Fe concentration in precursors, influencing the iron amount in MFI framework.

4.4.2.1 Effect of aging time

To investigate the effect of aging time, the heating temperature and time were fixed at 150°C and 10 h, respectively. Moreover, the iron concentration was fixed at 0.01 mole ratio of $FeCl_3$. SEM results of samples aged at various times are shown in Figure 4.4. When the mixture was aged for 36 h, the amorphous phase was obtained. As increasing the aging time to 60 h, no amorphous phase was observed, resulting in fully grown crystals. The crystal size was decreased as aging time was further increased due to more nucleation growth. However, the crystal sizes were not significantly different at the aging time between 84 to 132 h.

To confirm the SEM results XRD analysis was performed and indeed showed a broad amorphous peak at $2\theta = 23°$ (see Figure 4.5) when aging the sample for 36 h. The broad amorphous XRD peak disappears when the sample was further

aged for 60 h. In addition, the DR-UV results shown in Figure 4.6 indicate only intense charge-transfer transitions in the 220-245 nm ultraviolet regions, which are the characteristic range of the incorporated iron in the MFI framework, not extra-framework.

XRF analysis was used to confirm the total amount of Si and Fe in the zeolite (both inside and outside the framework), as listed in Table 4.1. The Si/Fe ratio (in calcined samples) decreases as the aging time increases to 84 h, and then increases again probably due to the limitation of MFI structure allowing certain amount of iron to be incorporated. It can be noticed that the iron content is lower than the actual loading in every conditions.

4.4.2.2 Effect of heating temperature

From previous study of the aging time effect, the 84 h aged sample gave homogeneous crystals of MFI, and also provided the highest amount of iron in the solid sample. Thus, for the study of the heating temperature effect, the aging and heating time were fixed at 84 and 10 h, respectively. It is known that increasing temperature not only affects to the growth rate and the product morphology [3], but also enhances condensation of transition metal. SEM (Figure 4.7) and XRD (Figure 4.8) results show only crystalline phase after heating at 130°C. The crystal size is increased as increasing the heating temperature due to an increase in the growth rate. Moreover, Figure 4.9 illustrates the increase of absorbance peak in the range of 200-245 nm ultraviolet regions, assigned to the Fe^{3+} in tetrahedral environment when the heating temperature is increased. However, Table 4.2 shows the decrease of the Si/Fe ratio of solids when the temperature is increased. The results indicate that the increase in temperature can increase the condensation of Fe into MFI structure [9]. However, at the temperature of 170°C, the Si/Fe ratio is increased possibly due to the degradation of the template molecule [7].

4.4.2.3 Effect of heating time

To obtain fully-grown crystals and highest amount of iron incorporated in MFI structure, the aging time and heating temperature were observed at 84 h and 150°C, respectively. In this study, the heating time was varied from 5 to 20 h by using the microwave technique. The SEM results shown in Figure 4.10 resulted in an

increase in Fe-MFI crystal size with heating time. In addition, the MFI pattern of Fe-MFI crystal confirmed by XRD results shows crystalline phase, see Figure 4.11. However, DR-UV results (Figure 4.12) indicate that at the heating time of 15 and 20 h gave a lower absorbance intensity of the incorporated iron in the MFI framework than 10 h heating time. The reason may be that some iron can not tolerate at these conditions of long heating, thus was released from the structure and became extra-framework. The Si/Fe ratio after 15 h heating thus maintained no effect (Table 4.3). As a summary, the heating time of 10 h was the optimal time, resulting in the highest amount of iron incorporated in MFI.

4.4.2.4 Effect of iron concentration

Fe loading effect on the crystal morphology was studied at the Si/Fe ratio of 100, 50, 33, 25, 20 and 16 while fixing the aging time for 84 h at room temperature and microwave heating at 150°C for 10 h. Figure 4.13 shows the change in morphology of crystals due to the change in iron content, illustrating the cubic shape of the crystals. As increasing iron loading, the shape of crystal becomes rounder and non-homogeneous [4] due to the difference in size between iron and silicon atoms. Therefore, the MFI crystals were distorted. However, at the Si/Fe ratio of 16, the amorphous phase was observed since the zeolite structure was collapsed. This was also confirmed by XRD analysis, giving a broad amorphous peak at 2θ = 23° (see Figure 4.14).

Table 4.4 shows that the amount of iron in calcined samples is almost the same as the amount of iron loaded. However the samples at the Si/Fe ratio of 100, 50 and 33 were white in color, while the samples at the Si/Fe ratio of 25, 20 and 16 were yellow-white, slight-yellow and yellow in color, respectively. This probably depicts the deposition of the extra-framework Fe outside the crystallites [10]. The ESR spectra (see Figure 4.15) of the samples at different Si/Fe ratios (loading) of 100, 50, 33, 25, 20 and 16 show two signals at g~4.8 and g~2 which are assigned to Fe^{3+} in lattice and cationic positions, and/or oxide of Fe (α-Fe_2O_3, γ-Fe_2O_3 and FeO(OH)), respectively. From these results, it can be confirmed that both framework and extra-framework Fe were together appeared in the Fe-MFI samples.

To quantitatively determine the distribution of framework and extra-framework Fe, the ion-exchange technique was conducted. The synthesized Na-Fe-MFI zeolite was exchanged with KNO_3 (0.1 M solution). The incorporation of iron in MFI framework can be determined from K^+/Fe ratio where K^+ is exchanged amount of K^+ ions and Fe is overall amount of Fe in zeolite. If the K^+/Fe ratio is equal to 1, all iron in the gel is incorporated into the crystalline lattice of zeolite, and for the ratio < 1, a fraction of iron should be located outside zeolite framework (Table 4.5).

Table 4.5 indicates the incorporation of iron into the zeolite lattice at various iron concentrations from the Si/Fe ratio equal to 100 to 20. The results show that, when Si/Fe at loading decreased, the amount of incorporated iron in the crystalline lattice was diminished. This incorporation was varied from 98 to 42%. The percentage of extra-framework Fe was approximately 36% for the Si/Fe ratio of 20 and 2% for Si/Fe ratio of 100.

4.4.3 Catalytic activity testing

The synthesized Fe-MFI samples at the Si/Fe ratio of 100, 33 and 20 were selected as representative catalysts to study their catalytic activity for selective catalytic reduction (SCR) of NO by CO. From the experiment, it was observed that the SCR of NO by CO did not occur by using all of the synthesized Fe-MFI catalysts. The synthesized Fe-MFI catalyst seemed not to be the appropriate catalyst for the NO reduction in these cases. However, CO conversion profiles for the synthesized Fe-MFI catalysts in CO + O_2 + NO reaction in Figure 4.16, illustrating as a function of reaction temperature from 50° to 450°C for the synthesized Fe-MFI catalysts at the ratio of 20 (curve a), 33 (curve b) and 100 (curve c), shows that at the Si/Fe ratio of 20, Fe-MFI catalyst provided the highest activity around 62.29% CO conversion at the temperature of 450°C. While the synthesized Fe-MFI catalysts at the ratio of 33 and 100 gave lower CO conversions of around 24.54 and 5.95%, respectively.

To study the effect of framework and extra-framework Fe in Fe-MFI zeolite, we impregnated a silicalite solid (MFI-structure type) with $FeCl_3$ salt solution. After impregnation, catalyst was dried at 120°C for 4 h and calcined at

550°C for 4 h in air. This catalyst was denoted as Fe_2O_3/silicalite, containing the same amount of iron as in the Fe-MFI sample having the Si/Fe ratio of 20. By this preparation method, there was only extra-framework Fe present in the sample [10]. Activities of pure silicalite (no Fe loading), Fe-MFI zeolite at the Si/Fe ratio of 20 and Fe_2O_3/silicalite were studied under the same conditions as indicated in the experimental part. It was found that, see Figure 4.17, CO conversion over Fe_2O_3/silicalite sample was lower than that over Fe-MFI zeolite at the Si/Fe ratio of 20. This lower activity could be due to the loss of Fe framework. However, the pure silicalite sample shows the lowest activity of CO + O_2 + NO reaction.

4.5 CONCLUSIONS

Fe-MFI zeolite was successfully synthesized via the sol-gel process and microwave technique, using silatrane and TPA as the precursor and template, respectively. The higher heating temperature is preferred for Fe-MFI synthesis due to the higher promotion of iron condensation into zeolite structure. However, this statement is limited by the degradation of the template molecule. In addition, the increase of aging and heating times promotes the increase of iron atom incorporated in the MFI structure. However, too long time decreases the incorporation of iron. All synthesized Fe-MFI zeolites contained irons in two different forms: framework and extra-framework. The fraction of framework Fe increased proportionally with increasing the Si/Fe ratios.

The synthesized Fe-MFI zeolite could not catalyze the reduction reaction of SCR of NO by CO. However, these catalysts could catalyze the oxidation of CO in this reaction. Moreover, framework and extra-framework Fe can catalyze CO oxidation reaction more than only extra-framework Fe does.

4.6 ACKNOWLEDGEMENTS

This research work was supported by the Postgraduate Education and Research Program in Petroleum and Petrochemical Technology (ADB) Fund,

Ratchadapisake Sompote Fund, Chulalongkorn University and The Thailand Research Fund (TRF).

4.7 REFFERENCES

1. Brabec, L., Jeschke, M., Klik, R., Nováková, J., Kubelková, L. and Meusinger, J. (1998). Appl. Cat. A: General, 170, 105-116.
2. Fejes, P., Kiricsi, I., Lázár, K., Marsi, I., Rockenbauer, A., Korecz, L., Nagy, J. B., Aiello, R. and Testa, F. (2003)., Appl. Cat. A: General, 242, 247-266.
3. Phiriyawirut, P., Magaraphan, R., Jamieson, A. M. and Wongkasemjit, S. (2003), Mater. Sci. and Eng. A, 361, 147-154.
4. Phiriyawirut, P., Magaraphan, R., Jamieson, A. M. and Wongkasemjit, S. (2003), Micro. and Meso. Mater., 64, 83-93.
5. Fernández-García M., Martínez-Arias A., Iglesias-Juez A., Hungría A. B., Anderson J. A., Conesa J. C. and Soria J. (2004), J. Catal, 214(2), 220-233.
6. Piboonchaisit, P., Wongkasemjit, S. and Laine, R. (1999), Science-Asia, J.Sci. Soc. Thailand, 25, 113-119.
7. Miyamoto, A., Medhanavyn, D. and Inui, T. (1986), Appl.Cat., 28, 83-103.
8. Huang, Y., -J., Wang, H.,.P. and Lee, J., F. (2003), Appl. Cat. B: Environmental, 40, 111-118.
9. Livage, J. (1998), Catal. Today, 41(1-3), 3-19.
10. Phu N. H., Hoa T. T. K., Thang H. V. and HA P. L. (2001), Appl. Cat. B: Environmental, 34, 267-275.

Table 4.1 Effect of aging time on the Si/Fe ratio of Fe-MFI samples determined using XRF analysis

Aging time (hour)	Si/Fe ratio (loading)	Si/Fe ratio (in calcined solids)
36	100	-
60	100	138
84	100	101
108	100	116
132	100	124

Table 4.2 Effect of the heating temperature on the Si/Fe ratio of Fe-MFI samples aged and heated for 84 and 10 h, respectively, using XRF analysis

Heating Temperature (°C)	Si/Fe ratio (loading)	Si/Fe ratio (in calcined solids)
110	100	118
130	100	115
150	100	101
170	100	140

Table 4.3 Effect of the heating time on the Si/Fe ratio of iron-MFI samples aged for 84 h and heated at 150°C using XRF analysis

Heating Time (hour)	Si/Fe ratio (loading)	Si/Fe ratio (in calcined solids)
5	100	113
10	100	101
15	100	136
20	100	134

Table 4.4 Effect of iron concentration on the Si/Fe ratio of iron-MFI samples aged for 84 h and heated at 150°C for 10 h using XRF analysis

Si/Fe ratio (loading)	Si/Fe ratio (in calcined solid)	Color
100	101	White
50	52	White
33	35	White
25	26	Yellow-white
20	23	Slight-yellow
16	-	Yellow

Table 4.5 Ion-exchange over Fe-MFI zeolites

Sample	Si/Fe ratio	Overall Fe amount (%mmol)	K+ exchanged ion amount (%mmol)	K+/Fe	Fe intra-framework fraction (%)
1	100	13.48	13.20	0.98	98
2	50	59.55	41.70	0.70	70
3	33	47.40	28.23	0.60	60
4	25	61.84	29.46	0.48	48
5	20	67.81	28.45	0.42	42

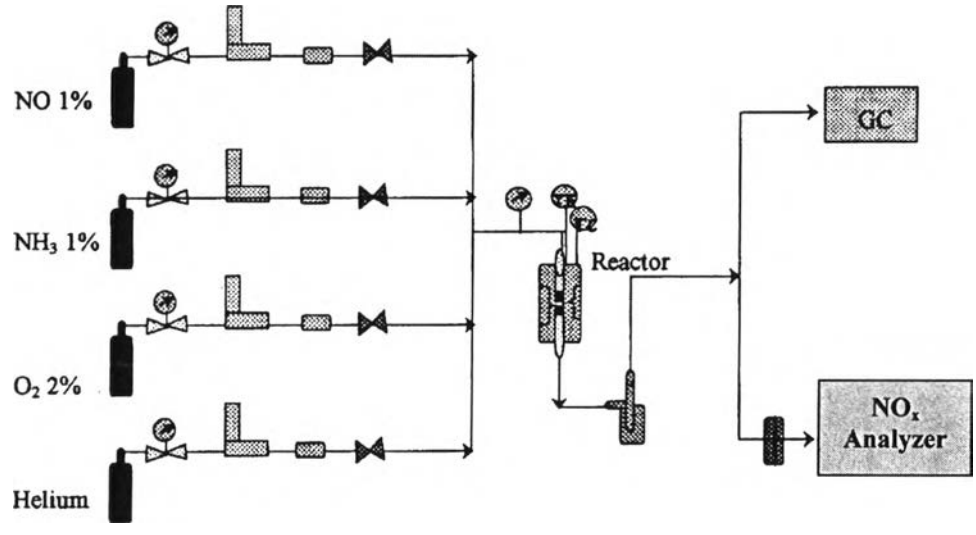

Figure 4.1 Schematic flow diagram of experimental equipments (Rochanutama *et al*, 2003).

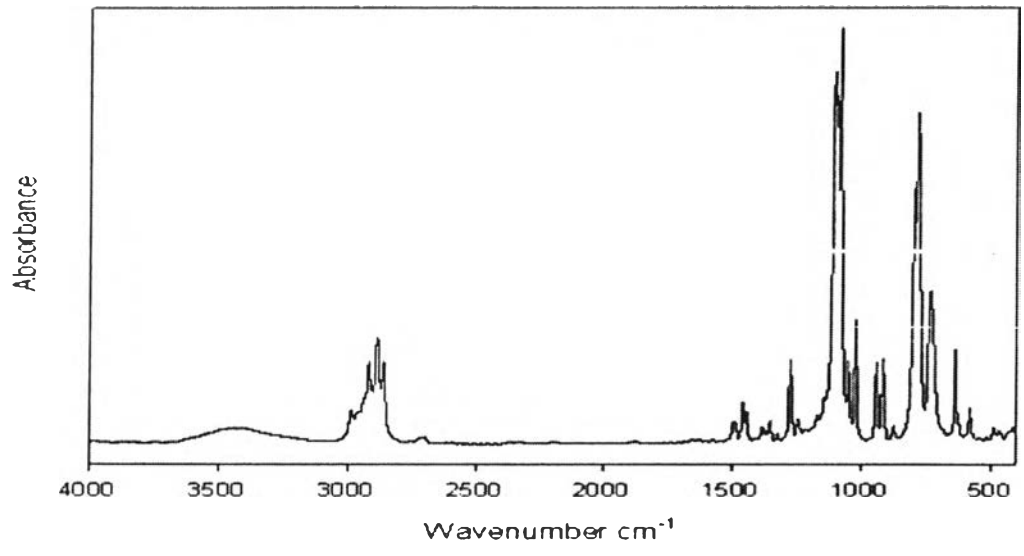

Figure 4.2 IR spectrum of silatrane.

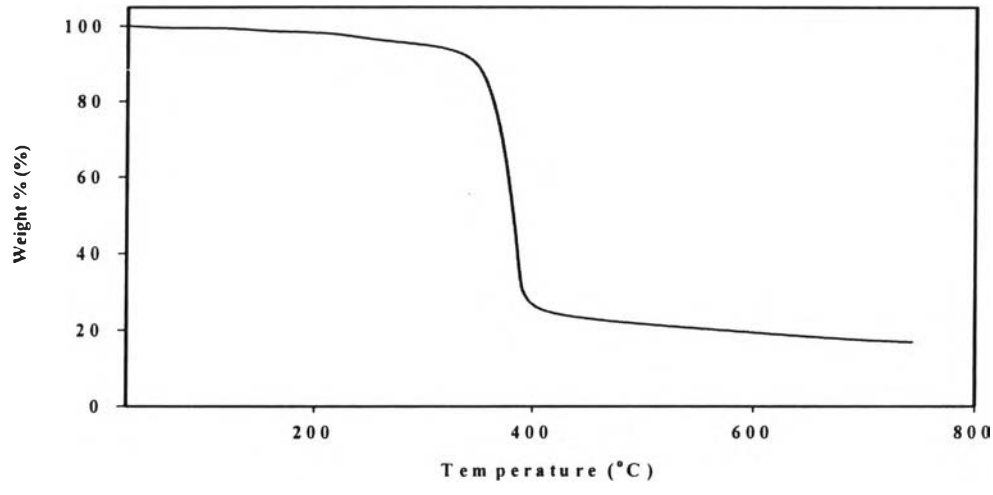

Figure 4.3 TGA analysis of silatrane.

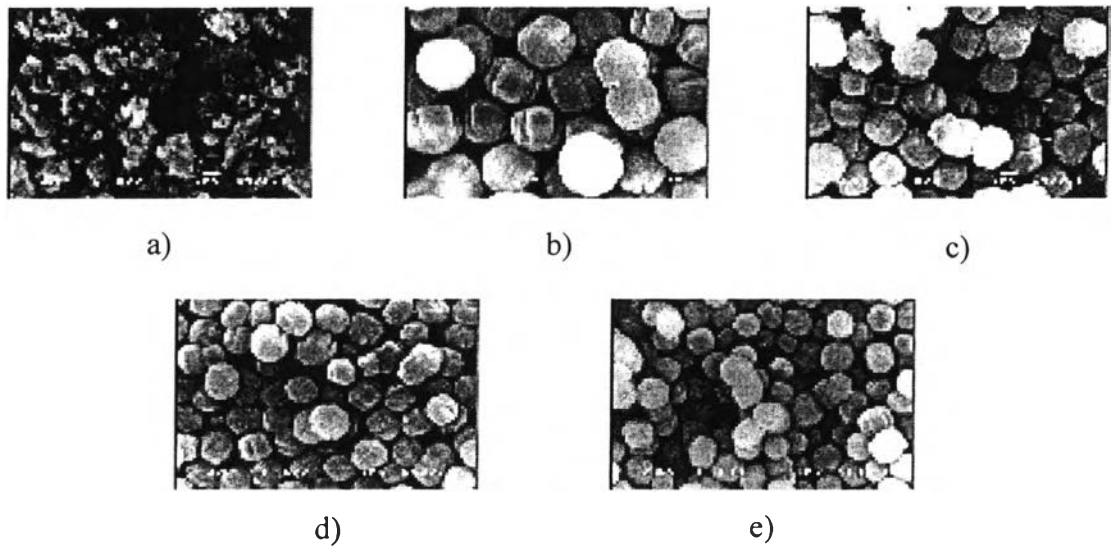

Figure 4.4 Effect of the aging time on the product morphology at 150°C for 10 h: (a) 36, (b) 60, (c) 84, (d) 108 and (e) 132 h.

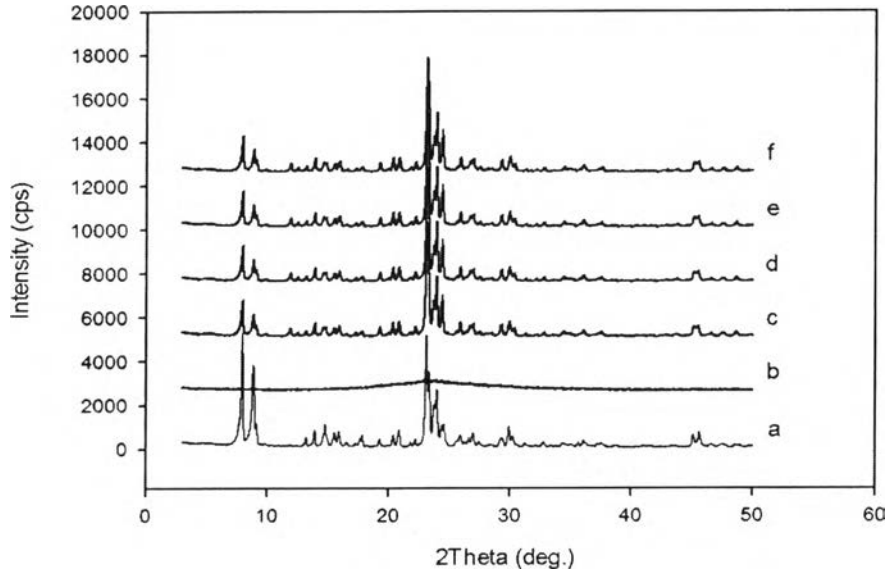

Figure 4.5 XRD spectra of Fe-MFI at various aging times: (a) MFI, (b) 36, (c) 60, (d) 84, (e) 108 and (f) 132 h.

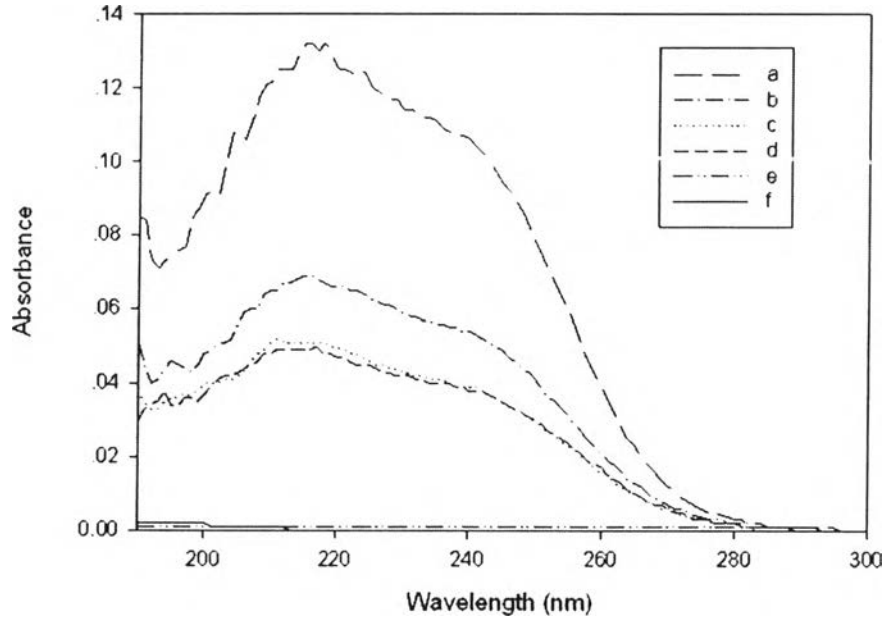

Figure 4.6 DR-UV spectra of Fe-MFI at various aging times of: (a) 108, (b) 84, (c) 60, (d) 132, (e) 36 and (f) MFI.

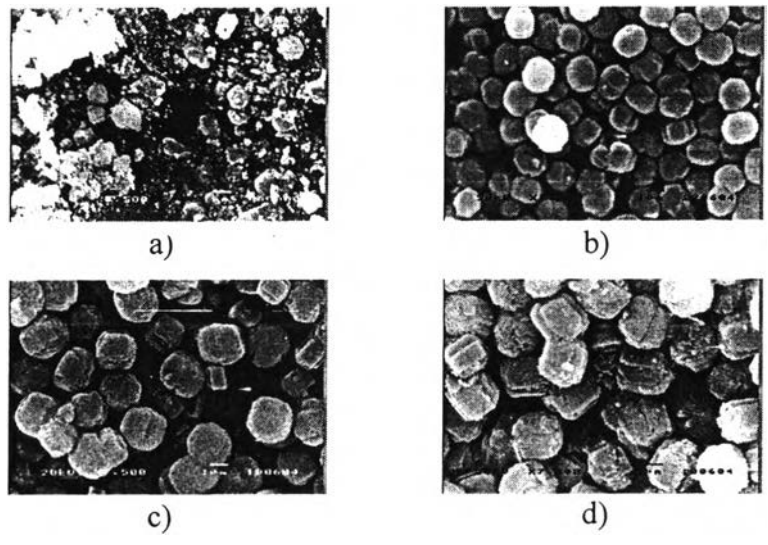

Figure 4.7 Effect of heating temperature on the product morphology with aging and heating times of 84 and 10 h, respectively: (a) 110°, (b) 130°, (c) 150° and 170°C.

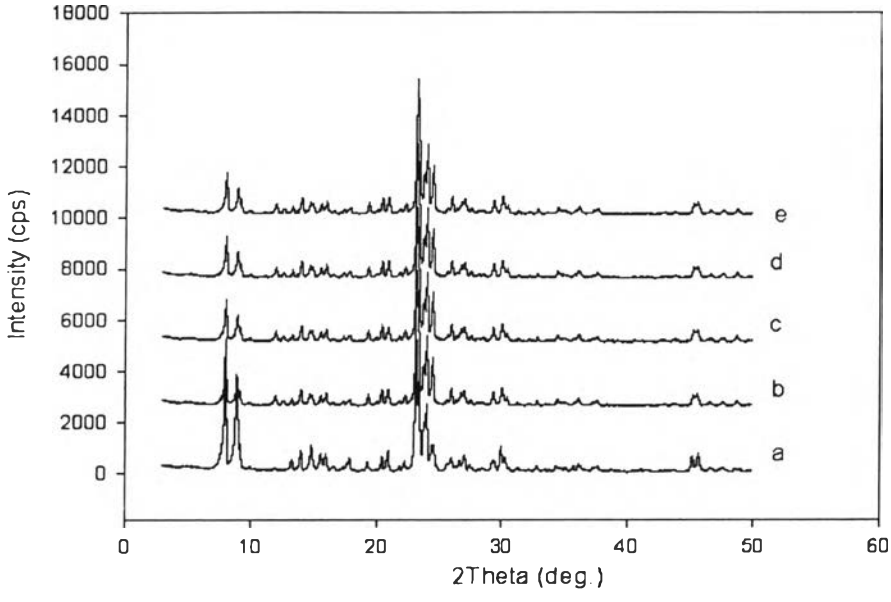

Figure 4.8 XRD spectra of Fe-MFI at various heating temperatures: (a) MFI, (b) 110°, (c) 130°, (d) 150° and (e) 170°C.

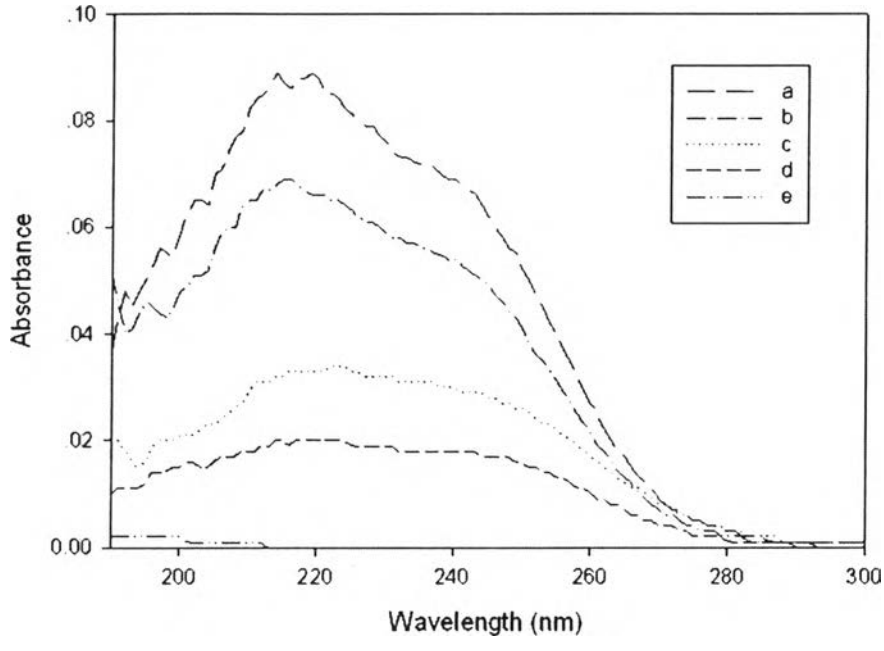

Figure 4.9 DR-UV spectra of Fe-MFI at various heating temperatures: (a) 170°, (b) 150°, (c) 110°, (d) 130°C and (e) MFI.

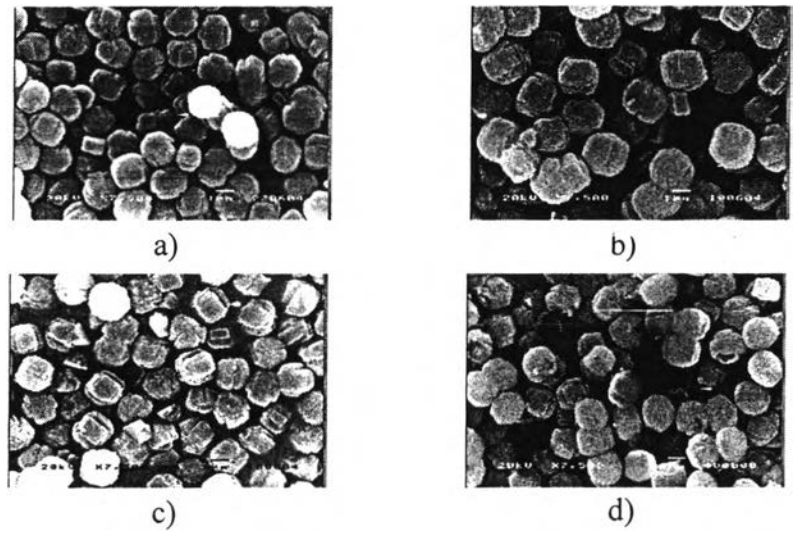

Figure 4.10 Effect of heating time on the product morphology with aging for 84 h and heating at 150°C: (a) 5, (b) 10, (c) 15 and (d) 20 h.

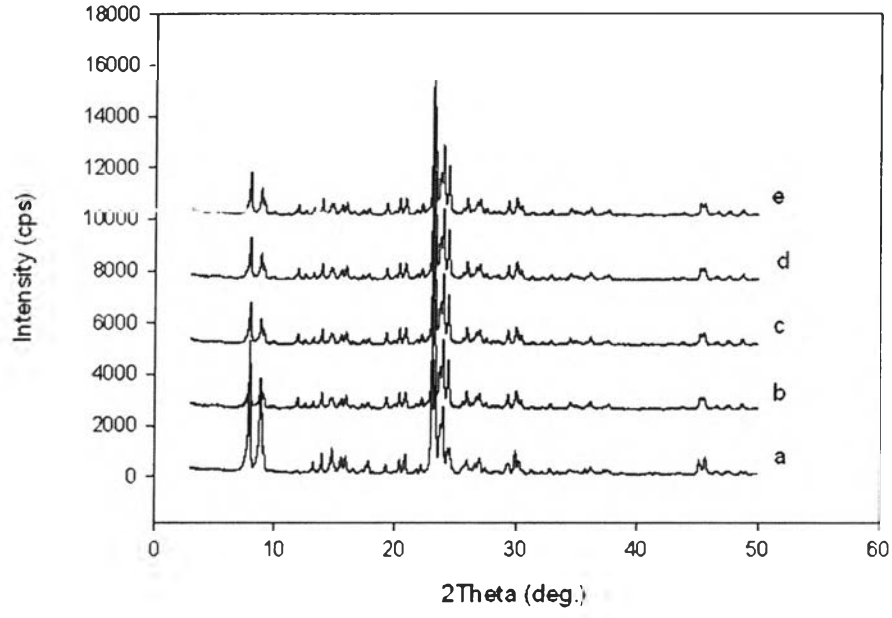

Figure 4.11 XRD spectra of Fe-MFI at various heating times: (a) MFI, (b) 5, (c) 10, (d) 15 and (e) 20 h.

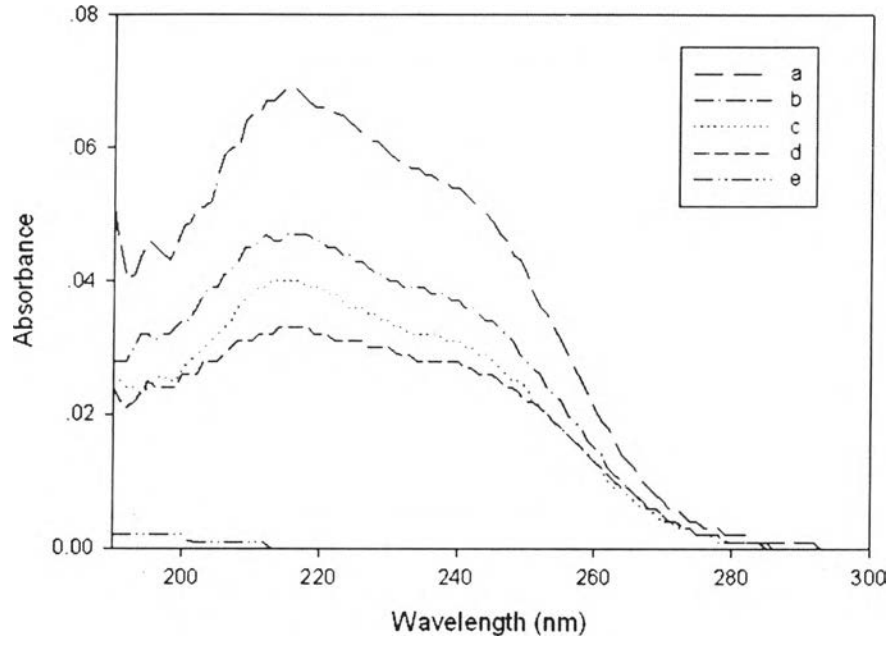

Figure 4.12 DR-UV spectra of Fe-MFI at various heating times: (a) 10, (b) 20, (c) 15, (d) 5 h and (e) MFI.

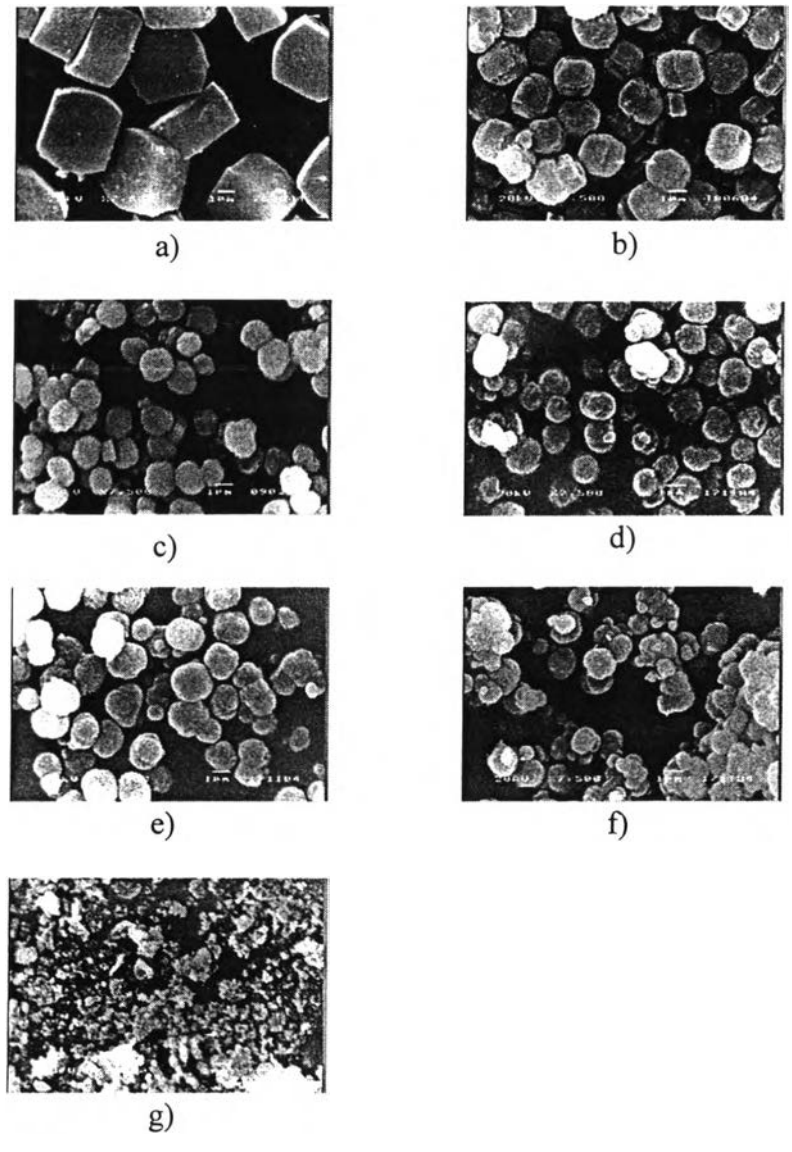

Figure 4.13 Effect of the iron concentration at various Si/Fe ratios on product morphology aged at room temperature for 84 h, and heated at 150°C for 10 h: (a) MFI: (b) 100, (c) 50, (d) 33, (e) 25, (f) 20 and (g) 16.

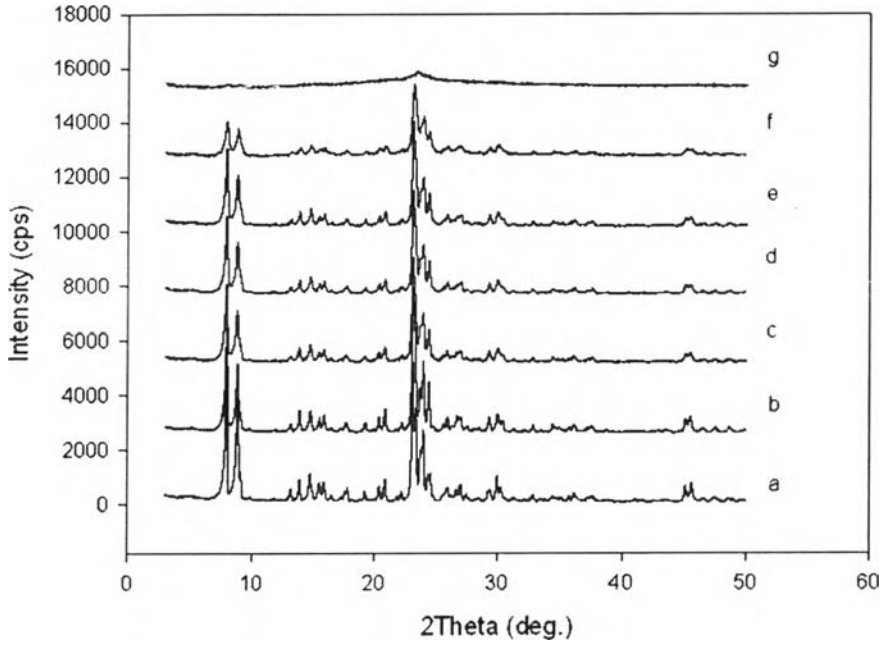

Figure 4.14 XRD sprectra of Fe-MFI at various Si/Fe ratios: (a) MFI: (b) 100, (c) 50, (d) 33, (e) 25, (f) 20 and (g) 16.

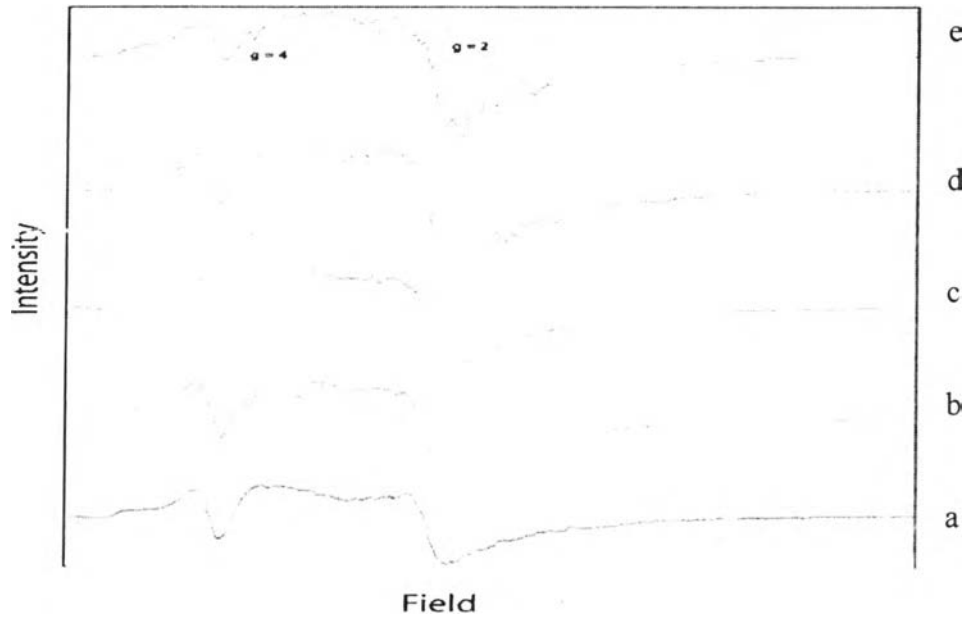

Figure 4.15 ESR spectra of Fe-MFI at various Si/Fe ratios: (a) 100, (b) 50, (c) 33, (d) 25 and (e) 20.

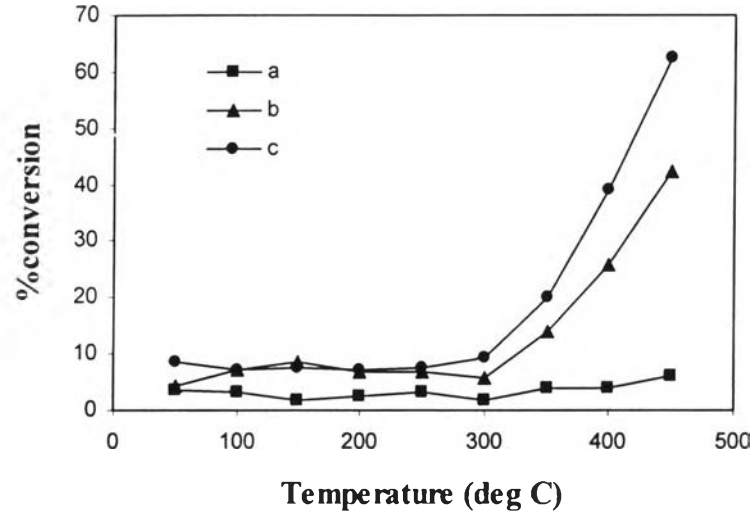

Figure 4.16 CO conversion profile for the SRC of NO by CO over Fe-MFI at various Si/Fe ratios: (a) 100, (b) 33 and (c) 20.

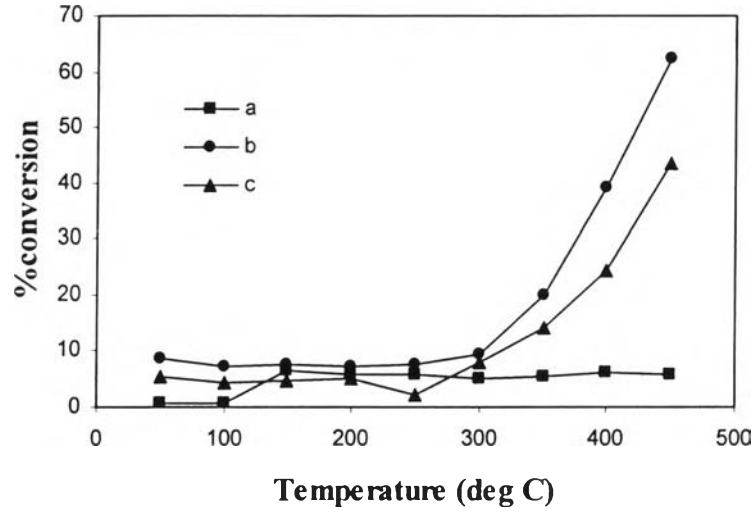

Figure 4.17 CO conversion profiles for the SRC of NO by CO over: (a) pure silicalite, (b) Fe-MFI at the Si/Fe ratio of 20 and (c) Fe_2O_3/silicalite.